



EOG-based eye tracking protocol using baseline drift removal algorithm for long-term eye movement detection

Jaehwan Ryu^a, Miran Lee^b, Deok-Hwan Kim^{c,*}

^a Technical Research Institute, SAMMI Information System, Seoul 08502, Republic of Korea

^b Graduate School of Information Science and Engineering, Ritsumeikan University, Shiga 5238577, Japan

^c Department of electronic engineering, Inha University, Incheon 402-751, Republic of Korea



ARTICLE INFO

Article history:

Received 23 March 2018

Revised 17 March 2019

Accepted 16 April 2019

Available online 24 April 2019

Keywords:

Human-computer interaction

Ubiquitous computing

Pattern recognition

Signal processing systems

Electrooculography

ABSTRACT

This paper presents a new method to remove baseline drift and noise by using a differential electrooculography (EOG) signal based on a fixation curve (DOSbFC) and a new electrode positioning scheme based on eyeglasses for user convenience. In addition, a desktop application and mobile applications to control the human-computer interface were implemented. Finally, we created experimental EOG eyeglasses and a new detection protocol using the proposed method for long-term step-by-step detection of eye movements and user comfort. The proposed DOSbFC calculates the difference values of accumulated EOG signals between the initial eye movement and fixation time. It allows long-term detection of eye movements with high accuracy and only requires a single calibration. The vertical and ground electrodes of the standard electrode positioning scheme caused discomfort of subjects; the proposed electrode positioning scheme solves these problems and enables the use of existing eyeglasses without design modification. The experimental results demonstrated that the average accuracy of the long-term eye movement detection was 94%, whereas those of the band pass filter and wavelet transform were 61% and 64%, respectively. This was because baseline drift and noise were removed by averaging the signal variations. Further experimental results demonstrated that the average information transfer rate of the proposed method was 6.0, whereas those of the band pass filter and wavelet transform were 1.1 and 0.9, respectively.

© 2019 Elsevier Ltd. All rights reserved.

1. Introduction

RECENTLY, numerous studies regarding human-computer interfaces using eye movement have been conducted (Barbara, Camilleri, and Camilleri (2019); Rahman, Bhuiyan, & Hassan, 2018; Wu et al. (2013); Wu et al., 2015; Yu, Lee, & Kim, 2012; Zhang, Yin, & Wang, 2015; Bulling, Ward, Gellersen, & Troster, 2011). The attention span, saliency, visual memory, and perceptual learning of the user can be determined from eye movements (Deng, Hsu, Lin, Tuan, & Chang, 2010; Barea, Boquete, Rotega, Lopez, & Rodriguez-Ascariz, et al., 2012). In addition, eye movements can be used to generate commands to control devices (Fernandez, Augusto, Seepold, & Madrid, 2012; Ianez, Ubeda, Azorin, & Perez-vidal, 2012; Liang et al., 2015; Manabe, Fukumoto, & Yagi, 2015). The most popular methods to track eye movements use video oculography (VOG) based on an infrared camera, a red-green-blue camera, and images. Another method used for eye tracking is electrooculography (EOG). EOG measures the movement of the eye via the

voltage difference between the cornea and retina (Brown et al., 2006). Therefore, EOG is relatively economical, and powerful, and has a simple acquisition approach with a fast user response. In addition, the EOG signal can directly recognize the user's intention because it is a biosignal (Postelnicu, Girbacia, & Talaba, 2012). Besides, the EOG signal is convenient for the user as the position of the attached electrodes for EOG is similar to the frame of a pair of eye goggles (Ianez, Azorin, & Perez-vidal, 2013; Yamagishi, Hori, & Miyakawa, 2006; Kirbis & Kramberger, 2009; Estrany, Fuster, Garcia, & Luo, 2008). Therefore, many studies regarding device control using biosignals adopt EOG signals. For example, Ianez et al. (2012) proposed an assistive robot application using radiofrequency identification and EOG. The present study uses a portable wireless EOG to control the robot arm.

Studies using EOG signals must solve the baseline drift problem. The baseline of an EOG signal varies continuously with time owing to baseline drift (Yu et al., 2012; Bulling et al., 2011; Estrany et al., 2008; Yagi, Kuno, Koga, & Mukai, 2006). The baseline may be changed by other neural signals and small movements of other body parts and most baseline drift is unrelated to eye movements. Therefore, previous studies measured EOG signals over a short period, fixed the head of the subject and repeated the calibration

* Corresponding author.

E-mail address: deokhwan@inha.ac.kr (D.-H. Kim).

for long-term activity analyses using EOG signals, or remove baseline drift using signal transformations (Bulling et al., 2011; Manabe et al., 2015). For example, Bulling et al. (2011) proposed a wavelet transform and bandpass filter (BPF) to resolve this baseline drift problem.

In addition, many design studies have been conducted to improve the portability of the device control using EOG signals (Wu et al., 2015; Bulling, Roggen, & Troster, 2009; Ianez et al., 2013). Bulling et al. (2009) proposed wearable EOG goggles and the analysis of the eye motion. This study forms a baseline for eye movement analysis in everyday environments and new forms of context awareness not possible currently (Bulling et al., 2009). Ianez et al. (2013) proposed the computer control of EOG eyeglasses. However, the user interface design is constrained as the electrodes to recognize vertical eye motion are located above and below the sides of the eye. Many wearable eye trackers using EOG signals are developed to be worn on the entire face or eye. Therefore, the existing eye tracker using EOG signals has mostly been used for research as the design is poor and the device is uncomfortable. Many subjects felt discomfort when attaching the electrode of the vertical EOG signal for a long time as the lower electrode is fixed to the adipose tissue of the cheekbone. In addition, it is not possible to downsize and commercialize the EOG signal acquisition device as the position of the electrodes is arranged around the eye. Thus, it is necessary to resolve the baseline drift problem of the eye tracker using EOG signals and relocate the electrode positions for user convenience and comfort.

This paper proposes a new electrode positioning scheme based on eyeglasses, and a differential EOG signal based on a fixation curve (DOSbFC) to remove baseline drift. With the DOSbFC, difference values of EOG signals are measured at the time of fixation. It then recognizes eye movements based on these difference values. The application transmits predefined commands based on classified eye movements. In addition, the new electrode positioning scheme is designed to be attached to the frame of commercial eyeglasses.

2. Background

2.1. EOG signal

The EOG signal is divided into horizontal and vertical signals, according to the position of the electrodes. A detailed description of the electrode positions is presented in Section 3.1. When the subject's gaze is forward (0°), the baseline of the EOG signal can be measured. Generally, the baseline is zero. An EOG signal has a linear relationship between the visual angle and the amplitude of the signal (Yu et al., 2012; Bulling et al., 2011; Bulling et al., 2009; Barea, Boquete, Mazo, & Lopez, 2002; Ianez et al., 2012; Liang et al., 2015; Manabe et al., 2015; Ianez et al., 2013; Yamagishi et al., 2006). Therefore, it is possible to analyze eye movements quantitatively. Different types of eye movement are classified as blinking, fixation, and saccade (Fig. 1).

2.2. Eye movement - saccade and fixation

Saccade refers to the act of moving the line of sight from the current focus of attention to another object (Yu et al., 2012; Deseilligny, Muri, Ploner, Gaymard, & Pechoux, 1995). Saccade occurs over short periods of 10–100 ms, unlike smooth pursuit (slow eye movement) (Yu et al., 2012; Huaman & Sharpe, 1993). The maximum detection range of horizontal and vertical saccade is approximately 45° and 40° , respectively. Fixation can be described as the situation in which eye movement stops for approximately 150–200 ms between two saccades (Yu et al., 2012; Deseilligny et al., 1995; Huaman & Sharpe, 1993). Fixation refers to the fixation of

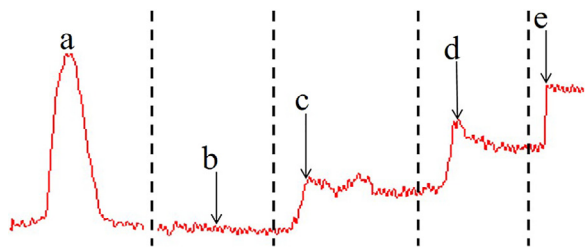


Fig. 1. Vertical EOG signals for five types of eye movement: (a) blink, (b) eye fixation and 0° saccade, (c) 0° – 10° saccade, (d) 10° – 20° saccade, and (e) 20° – 30° saccade.

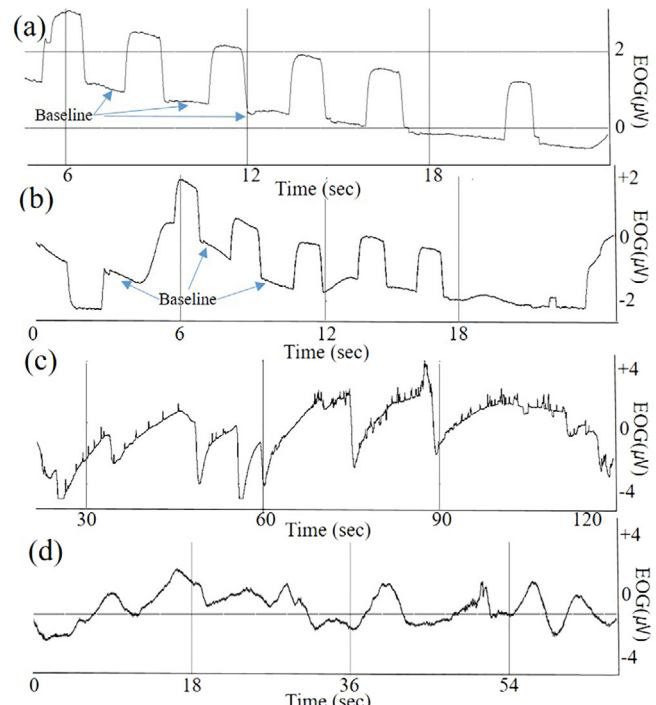


Fig. 2. Examples of baseline drift: (a) linear (repeated five times, upward 30° saccade), (b) non-linear (repeated five times, upward 30° saccade), (c) wavering (single blink), and (d) oscillating (no movement).

the eyeball to focus and fixation time refers to the time to focus after stopping the eyeball.

2.3. Eye movement - blinking

When a subject blinks, eyelids are closed and there is a simultaneous retraction of the eyeball. The eyelid then opens (Riggs, Kelly, Manning, & Moore, 1987). A blink lasts approximately 100–150 ms, and the average eye movement range is approximately 30° (Manabe et al., 2015). Thus, a blink can be measured using vertical signal components of EOG signals. Typically, a person blinks 20–30 times per minute (Yu et al., 2012; Huaman & Sharpe, 1993).

2.4. Baseline drift

Baseline drift in an EOG signal poses the greatest difficulty for the visualization of the correct waveform and computerized detection of wave complexes based on threshold decisions (Yu et al., 2012; Bulling et al., 2011; Estrany et al., 2008; Yagi et al., 2006). In addition, baseline drift is a slow signal change superposing on the EOG signal, and is mostly unrelated to the eye movement (Bulling et al., 2011). Fig. 2 shows an example of baseline drift

when a 0.1–10 Hz hardware BPF and a 60 Hz notch filter are applied to an EOG signal. It shows four types of baseline drift: linear, non-linear, wavering, and oscillating. Several approaches have been proposed to remove baseline drift from electrocardiography (ECG) signals and these methods have been used in off-line pre-processing of ECG signals (Tinati & Mozaffary, 2006; Chouhan & Mehta, 2007). Because ECG has repetitive signal characteristics, these algorithms perform adequately after removing the baseline drift (Bulling et al., 2011). However, for an EOG signal with no repetitive characteristics, the existing algorithms for baseline drift removal cannot be applied. Previous studies using an EOG signal presented a wavelet transform and BPF to resolve this baseline drift problem (Bulling et al., 2011) and these methods are efficient. However, if the baseline is changed substantially, these methods are not suitable. In addition, the recognition rate drops as the original signal may be distorted.

2.5. Denoising

Noise in EOG signals is caused by the residential power line, usually referred as mains hum, measurement circuitry, electrodes, wires, and other physiological sources of interference. The noise of EOG signals cannot be predicted and corrected as there is no repetitive reference signal and pattern, unlike ECG and electromyography. The denoising algorithm of EOG signals should preserve its characteristics to enable saccade recognition and eye movement analysis. Denoising algorithms must not introduce artificial signals that may accidentally be interpreted as saccades during signal processing (Bulling et al., 2011). Therefore, the denoising algorithm of EOG signals employs a method to reduce noise using neighboring characteristics without changing the signal, such as a median filter, high pass filter, low pass filter, wavelet, and moving average filter.

3. Proposed method

This paper proposes a DOSbFC method to remove baseline drift and noise, and activity recognition using an EOG signal to control a PC, notebook, tablet, and smartphone. In addition, the electrode mounting positions are relocated to adapt to eyeglass-shaped consumer electronics. Fig. 3 shows the flow chart of the proposed method for (a) initial calibration and (b) activity recognition of eye movements using EOG signals.

In the first step, the initial calibration was performed to measure a subject's initial baselines for horizontal and vertical EOG signals. The user-specific voltage values corresponding to a 1° angle eye movement in four directions: left, right, up, and down, were measured. This calibration was performed separately from processing the chain of input EOG signals. Even in the horizontal or vertical EOG signal and subject, there is a user-specific difference in voltage values between positive and negative signal due to differences in the shape of the eyeball, ocular voltage and biological characteristics. Therefore, we calculated the user-specific voltage for each of the four directions per subject.

In the second step, for two-input EOG signals capturing the horizontal and the vertical eye movement components, the DOSbFC was performed to remove baseline drift and noise. In the third step, four activities were analyzed to detect eye movements, namely blinks, horizontal saccades, vertical saccades, and fixation. When a saccade or blink was detected, the voltage values of contiguous input EOG signals were recorded sequentially, and their voltage amplitudes calculated after detecting the fixation. The range of the eye's gaze (10°, 20°, and 30°), were analyzed by comparing the voltage amplitudes of the input EOG signals with the corresponding calibration values. In many studies, the EOG signal guarantees linearity up to 30° (Simini, Touya, Senatore, & Pereira, 2011). We limited the saccades detection range to 30° ($\pm 5^\circ$) to

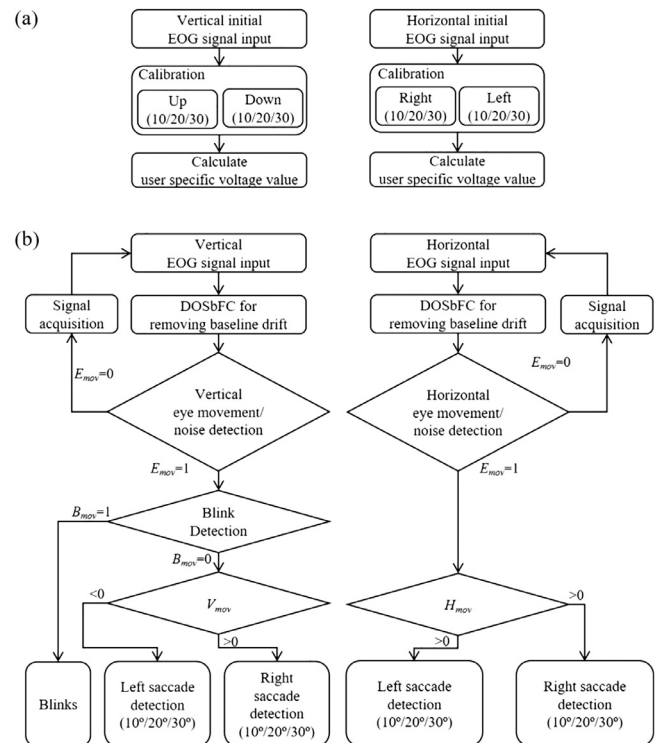


Fig. 3. Flow chart of the proposed method: (a) initial calibration and (b) activity recognition of the eye movement using EOG signals.

minimize the linearity error of the EOG signal. In addition, we did not consider moving and other bio signal noise at this calibration step, because the subjects participating in the experiment sat in a fixed position and viewed the screen as a frontal gaze.

The EOG electrode positioning schemes are shown in Fig. 4: (a) standard positioning, (b) proposed positioning, (c) wearing glasses using the proposed positioning (front view), and (d) wearing glasses using the proposed positioning (side view).

3.1. Electrode positioning scheme based on eyeglasses

The electrode mounting positions were relocated for user convenience. The standard EOG electrode positioning scheme was designed to improve the accuracy of eye tracking, but this is generally uncomfortable for the user (Bulling et al., 2009; lanez et al., 2013). In the standard EOG electrode positioning scheme, which positions the electrodes around the eye, makes this arrangement amenable to being mounted on eyeglasses, with two horizontal electrodes placed on the right and left of the eyes and two vertical electrodes placed above and below the eye. Therefore, the device control using EOG signal is less popular than other bio signals owing to the difficulty in bionic engineering and commercial design.

To solve this problem, we propose a new electrode positioning scheme based on eyeglasses (Fig. 4). A minimum of five electrodes were relocated to adapt to the structure of the frame of the eyeglasses. Two vertical electrodes were mounted on the nose pad and the bridge of the eyeglasses. Two horizontal electrodes were placed between the temple and skin contact point of the eyeglasses. A ground electrode was placed between the eyeglasses tip and the mastoid contact point. In this positioning scheme, normal eyeglasses can be used without design modification as the EOG electrodes can be hidden by the frame. However, the proposed electrode arrangement is not entirely original in all its aspects. Specifically, a few labs are developing commercial eye track-

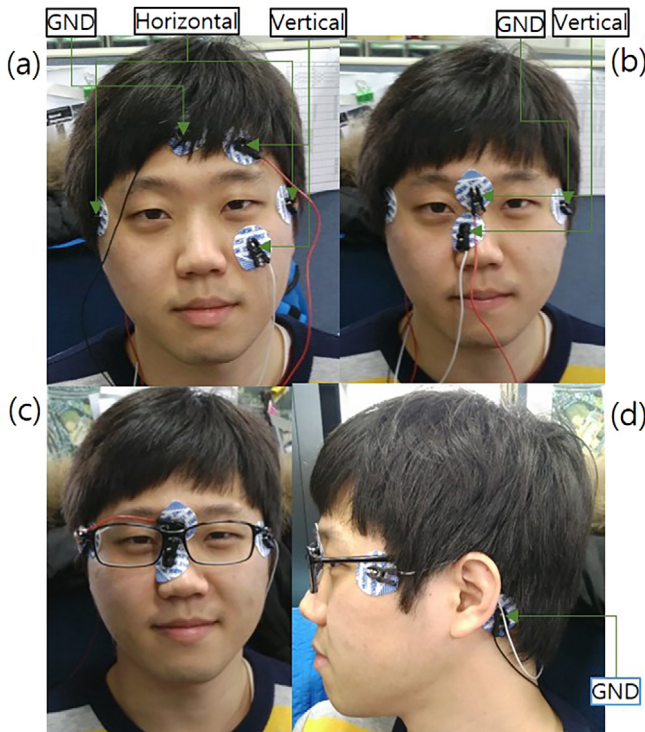


Fig. 4. EOG electrode positioning scheme: (a) standard positioning scheme, (b) proposed positioning scheme, (c) wearing glasses using the proposed positioning scheme (front view), and (d) wearing glasses using the proposed positioning scheme (side view).

ers using EOG signals. Such EOG glasses have been developed by IMEC and the Japanese eyewear manufacturer JINS (Draper., 2018; Kunze and Tanaka, 2014). Both products have improved the convenience by modifying the electrode placement based on glasses.

3.2. Differential EOG signal based on fixation

A new DOSbFC method is proposed to remove baseline drift and noise, and detect eye movements using an EOG signal to control mobile human-computer interface applications. Generally, when gazing at an object in front, the EOG signal should have a reference voltage of 0V. However, the baseline drifts due to changes in the ground value, changes in body condition, etc. The proposed method allows long-term eye-movement recording, requiring only a single calibration. At the initial calibration, the subject-specific voltage values corresponding to movements of 10°, 20°, and 30° angles in four directions: left, right, up, and down were measured. This process was repeated five times and average voltage values were calculated. For the initial calibration, a subject was required to look at a spot located at a specified angle on the screen. Based on the linearity of the EOG signal, the voltage values at 1° increments for the four directions of the eye's gaze were calculated automatically. The time required to stop the eyeball movement following blinking or saccade is called fixation time. Depending on the subject, fixation times range from 150 to 300 ms. Herein, the fixation time was defined as a minimum time of 150 ms (Yu et al., 2012; Deseilligny et al., 1995; Huaman & Sharpe, 1993). It was measured during the initial single calibration in stage 2.

During the eye-based activity recognition stage, the horizontal and vertical input EOG signals were transformed into differential EOG signals to minimize baseline drift. Fig. 5 shows how the proposed difference model change the saccade amplitude compared to the original EOG. Fig. 5(a) shows the original EOG signal generated by the saccade. All measured EOG signals between initial

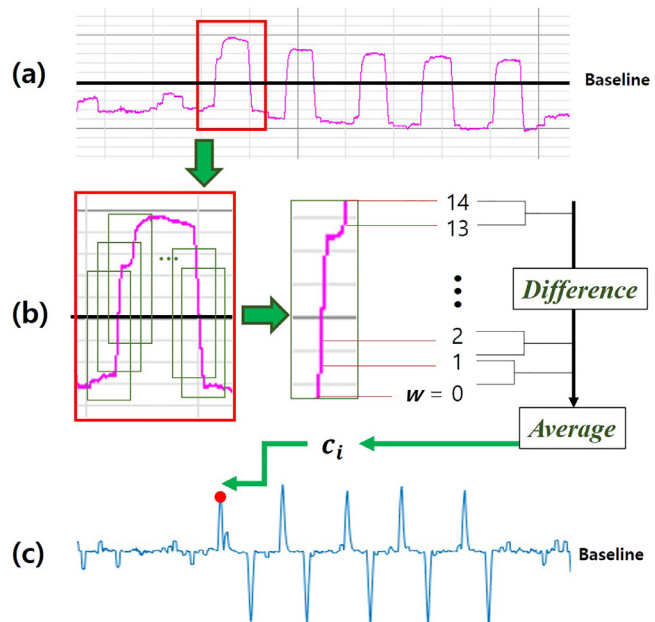


Fig. 5. (a) EOG signals, (b) f_i input signal and the difference values of the selected signals in sliding windows, (c) the converted DOSbFC signal c_i calculated by averaging the difference values of the selected EOG signals.

eye movement and fixed time were recorded. Since the fixation time for motion recognition is at least 150msec, the window size is set to include all EOG signals generated during 150msec to obtain the differential signal c_i for the i th input signal f_i . The sliding window was used to distinguish the start and end points of the input signals for real-time processing. Fig. 5(b) shows the differential signals calculated as the difference between the voltage amplitudes of the EOG signals separated by 10msec in the signals in one window, f_{i+1} and f_i , ..., f_{i+14} and f_{i+13} . We used a 10msec interval because the neuron activation time to generate the measurable synaptic potential is approximately 10msec and the minimum duration of the saccade movement is 10msec (Bulling et al., 2011; lanez et al., 2013). Fig. 5(c) shows the DOSbFC signal c_i obtained by averaging the difference signals in the window. In order to recognize the change of the saccade amplitude, the interval of the sliding window was set to 10msec. That is, the next difference signal c_{i+1} is gradually calculated using the EOG signals in the next window including the EOG signal f_{i+1} after 10msec. The differential EOG signal values were calculated using Eq. (1):

$$c_i = \frac{\sum_{w=0}^{(\text{fixation time} / 10 \text{ m sec})-1} (f_{i+(w+1)} - f_{i+w})}{\text{fixation time} / 10 \text{ m sec}} \quad (1)$$

where w is 0, 1, ..., 14 and represents the index value of the selected EOG signals at intervals of 10msec in the window and w was used to select the input signal within the sliding window. f_i is voltage amplitude of i th EOG signal. For f_i of each EOG signal, a voltage of a corresponding differential EOG signal c_i was calculated by averaging the difference values of the EOG signals between the initial eye movement and the fixation time. The proposed method selects and averages the most similar potentials within the range of the sliding window. It slides the window along the sample once to find the difference between the selected signals and average them to obtain the c_i signal. Next, the next interval is set, and a new potential set is selected and averaged. Sliding-window selective differential averaging is used instead of simply averaging signal differences. The averaging process is based on the selection of signal sections that have shapes similar to the various potentials of the sample set and uses a uniform weight of the selected po-

tential. The baseline of the differential EOG signals were proximal to the baseline (zero voltage) if sudden changes, such as saccades, did not occur, minimizing both baseline drift and noise owing to the moving average effect (Harun et al., 2009). Therefore, it can be used to trace eye gaze point coordinates.

By comparing the differential EOG signal with the user-specific voltage threshold of 1° eye movement in all directions, the eye movement or noise recognition was calculated using Eq. (2):

$$E_{mov} = \begin{cases} 0, & 5b_N \leq c_i \leq 5b_P \\ 1, & \text{otherwise} \end{cases} \quad (2)$$

where b_N is the subject-specific voltage (negative value) of a 1° eye movement in the left (down) direction with a horizontal (vertical) EOG signal, and b_P is the subject-specific voltage (positive value) of a 1° eye movement for the right (up) direction with the horizontal (vertical) EOG signal.

The EOG signals have a potential difference depending on the eyeball and electrode position. As the linearity of EOG signals in one direction is preserved, the positive and negative subject-specific voltage value must be measured for high precision recognition of a saccade. Therefore, we calculated b_P and b_N . Note that the voltage value of a 1° eye movement in each direction was calculated with a one-time calibration. A difference value within the given range indicates that there was no eye movement ($E_{mov} = 0$). Otherwise, eye movements were deemed to have occurred ($E_{mov} = 1$). This process was repeated for contiguous vertical and horizontal input EOG signals. We assumed that an eye movement with a visual angle lower than 5° was recognized as noise (Merino, Rivera, Gómez, Molina, & Dorronzoro, 2010).

3.3. Activity recognition using an EOG signal

Types of eye movement were classified as blink, fixation, and saccade. We used 12 variants of saccade (four directions: left, right, up, and down, and three amplitudes: 10°, 20°, and 30°). If E_{mov} became one, the proposed method calculates a summation of difference values, c_i , between the initial eye movement time and fixation time. This is because of the linear relationship between the EOG signal and eye gaze angle. Fig. 6 shows examples of eye movements denoted by the difference values of the EOG signals. In Fig. 6, the x-axis and the y-axis represent the time and voltage, respectively. The horizontal and vertical movements were recognized separately. We defined v as the vertical signal and h as the horizontal signal from the following formula. For example, the user-specific voltage value of 1° is b_{vN} . The vertical eye movement recognition consisted of two steps in the blink and up/down saccade recognition. In the first step of the vertical eye movement

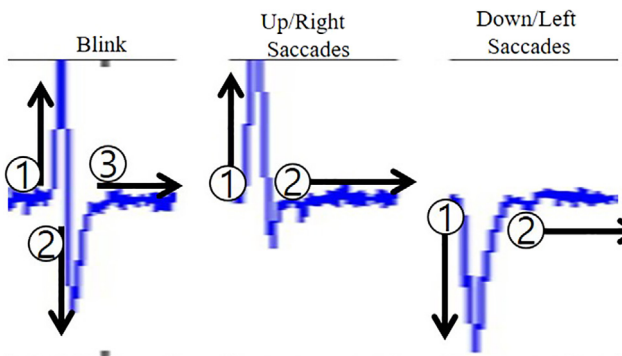


Fig. 6. Examples of eye movement denoted by different EOG signal values (the numbers in the circle are the eye movement pattern is in numerical order).

recognition, the blink recognition was calculated using Eq. (3):

$$B_{mov} = \begin{cases} 1, & \{5b_{vN} \leq P(c_v) + N(c_v) \leq 5b_{vP}\} \\ & \text{and } \{10b_{vP} \leq P(c_v)\} \\ 0, & \text{otherwise} \end{cases} \quad (3)$$

where b_{vP} is the user-specific voltage of the positive vertical EOG signals, and b_{vN} is the user-specific voltage of the negative vertical EOG signals, $P(c_v) = \sum_i^n c_{vi}$, if $c_{vi} > 0$, $N(c_v) = \sum_i^n c_{vi}$, if $c_{vi} < 0$, c_{vi} is the difference values of the vertical EOG signals calculated using (1), $v_i = 1, 2, \dots, n$, n is the number of input EOG signals from the time of the eye movement start ($E_{mov} = 1$) to the fixation time. We define that the sum of c_{vi} , where c_{vi} is a positive number, is equal to $P(c_v)$, and the sum of negative numbers c_{vi} is equal to $N(c_v)$. When a subject's eye blinks ($B_{mov} = 1$), the eyeball moves upward and downward, and then returns to its original position. In addition, if the angle of the eye movement was larger than 10°, it was detected as a blink ($B_{mov} = 1$). Otherwise, an up/down saccade occurred ($B_{mov} = 0$). If B_{mov} becomes one, then the vertical eye movement recognition ends. In the second step of the vertical eye movement recognition ($B_{mov} = 0$), the up/down saccade recognition was calculated using Eq. (4):

$$V_{mov} = \begin{cases} P(c_v)/b_{vP}, P(c_v) \geq |N(c_v)| \\ N(c_v)/b_{vN}, & \text{otherwise} \end{cases} \quad (4)$$

As shown in the up/down saccades in Fig. 6, when a subject has an up saccade eye movement, the eyeball moves upward/downward and then returns to its original position. As long as the subject does not intentionally move their eyeballs, the pattern of saccade is generated only in one direction. Therefore, we recognized the direction of the saccade by comparing the value of $P(c_v)$, and the absolute value of $N(c_v)$. If the $P(c_v)$ is greater than the $N(c_v)$, it is determined as an up saccade. Otherwise, it is determined as a down saccade. The up/down saccade calculated using (4) is expressed in degrees. $P(c_v)$ and $N(c_v)$ are the total eyeball movement distance, and b_{vP} and b_{vN} are the 1° user-specific voltage. Therefore, the angle of saccade was calculated by dividing the user-specific voltage and the larger of the two comparison values.

Furthermore, we recognized horizontal eye movements using the same method as applied for recognition of a vertical up/down saccade, using Eq. (5):

$$H_{mov} = \begin{cases} P(c_h)/b_{hP}, P(c_h) \geq |N(c_h)| \\ N(c_h)/b_{hN}, & \text{otherwise} \end{cases} \quad (5)$$

where b_{hP} is the user-specific voltage of the positive horizontal EOG signals, b_{hN} is the user-specific voltage of the negative horizontal EOG signals, $P(c_h) = \sum_i^n c_{hi}$, if $c_{hi} > 0$, and $N(c_h) = \sum_i^n c_{hi}$, if $c_{hi} < 0$, c_{hi} is the difference values of the horizontal EOG signals. When a subject has the right saccade eye movement, the different EOG signal values move upward and then return to their original position, as shown in Fig. 6. Following this saccade, an approximately 150 ms fixation occurs. If the angle of the eye movement is greater than +5° ($E_{mov} = 1$), it was detected as a right saccade with a horizontal EOG signal. When a subject has a left saccade eye movement, the different EOG signal values moved downward and then return to their original positions, as shown in Fig. 6. Following this saccade, an approximate 150-ms fixation occurred. If the angle of the eye movement was less than -5° ($E_{mov} = 1$), it was detected as a left saccade with a horizontal EOG signal. After a blink or saccade occurred, if the voltage returned to the baseline, the fixation was detected.

4. Desktop application controlling a human-computer interface using an EOG signal

4.1. Desktop application architecture

The desktop application controlling the human-computer interface was implemented for use on all desktop platforms (Fig. 7). In addition, the desktop application runs as a background process. The desktop application was developed based on the Microsoft .Net Framework. To improve performance and memory efficiency, the application was composed of four threads: input/output (I/O), main, control, and render threads. Multi-threaded configurations increase resource sharing efficiency and responsiveness, and enables code modularization. The I/O thread managed the input EOG signal and assisted EOG signal acquisition device in communicating with the desktop computer. It identified vertical, horizontal, and forward signals for queueing in the signal processing function block where the DOSbFC algorithm was implemented. The main thread controls the other three threads and recognized eye movements using the difference values of the EOG signals. The control thread issued commands to control the hardware, such as speakers, mouse, keyboard, as well as external applications. Lastly, the render thread managed the graphic interface, displaying the status and plotting input EOG.

4.2. Desktop application

The master and setting applications were implemented to control the human-computer interface using EOG signals, and they set the initial command and control levels. Fig. 8 shows the desktop master application and the desktop setting application. The master application (Fig. 8(a)) issued commands based on specified criteria by analyzing the input EOG signal. In addition, the command

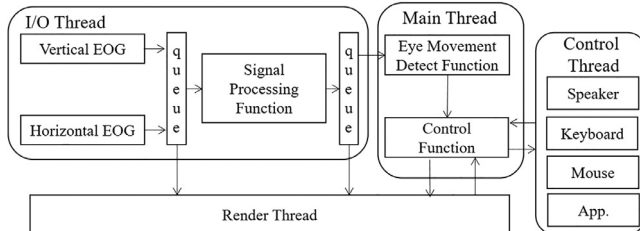


Fig. 7. Desktop application architecture.

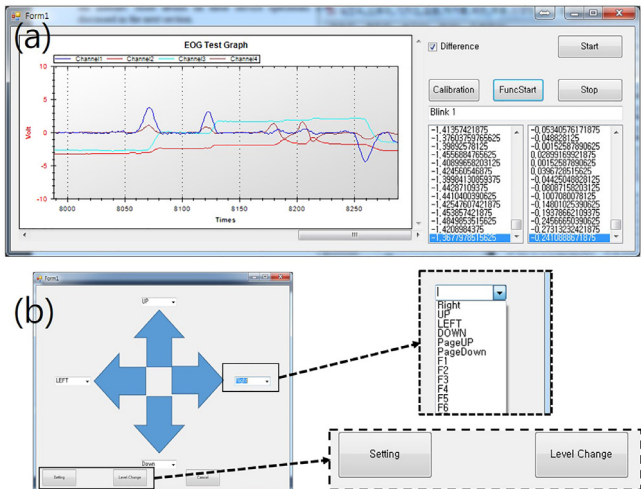


Fig. 8. Desktop application architecture: (a) desktop master application, and (b) the desktop setting application.

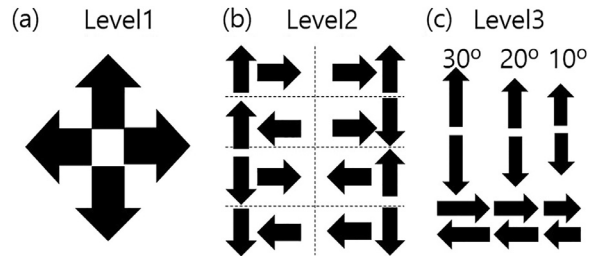


Fig. 9. Three control command levels: (a) command level 1, (b) command level 2, and (c) command level 3.

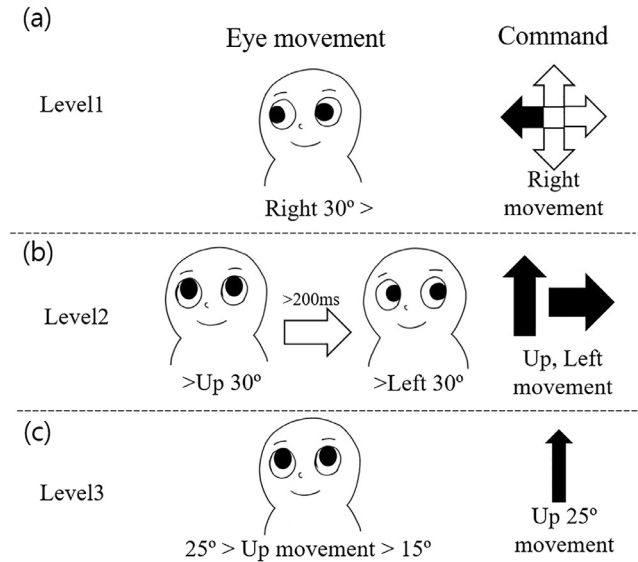


Fig. 10. Examples of generating commands: (a) right action in Level 1, (b) up and left action in Level 2, and (c) up action of 20° in Level 3.

was executed as an input/output device, according to the function set through the setting application when eye movement recognition was completed. Therefore, it can be used as a secondary controller in all Windows-based applications. An eye-protect function is implemented to prevent visual display terminal (VDT) syndrome (Yao, Davidson, Durairaj, & Gelston, 2011; Blehm, Vishnu, Khattak, Mitra, & Yee, 2005). The eye-protect function produced a warning message and beeped when it detected fewer than 10 blinks in one minute (a work-around to reduce VDT syndrome (Blehm et al., 2005)). The setting application set the start motion, type of command, and command level, as shown in Fig. 8(b). The start motion consists of a right click, middle mouse button click, double blink, and triple blink. Commands were divided into three levels in accordance with the type of action. Note that the commands can be configured using a ComboBox. Fig. 9 shows the three control command levels. As shown in Fig. 9(a), Level 1 had four actions in which the eyeball moves vertically or horizontally by more than 30°. In addition, Fig. 10(a) shows an example of generating a command using a right action in Level 1. As shown in Fig. 9(b), Level 2 had eight actions, in which the eyeball sequentially moved in the vertical and horizontal direction, or horizontal and vertical direction by more than 30°. In addition, Fig. 10(b) shows an example of generating a command using up and left actions in Level 2. Lastly, as shown in Fig. 9(c), Level 3 had 12 actions, in which the eyeball moved horizontally or vertically by 10°, 20°, and 30°. Fig. 10(c) shows an example of generating a command using an up action of 20° in Level 3. Control commands were executed when the eyeball returned to its original position within 300 ms of the action. Control commands did not use the eyeball diagonal action as it was

Table 1

Set commands according to applications (Level 1).

Application name	Desktop application	Text viewer, web viewer (Mobile)	Manga viewer, video viewer, gallery viewer (Mobile)	Mp3 player (Mobile)
Up	Page up	Scroll up	Next 10 pages	Volume up
Down	Page down	Scroll down	Previous 10 pages	Volume down
Left	Alt + ← (back key)	Previous page	Previous page	Previous music
Right	Alt + → (go key)	Next page	Next Page	Next music

Table 2

Set commands according to applications (Level 2).

Application name	Desktop application	Text viewer, web viewer (Mobile)	Manga viewer, video viewer, gallery viewer (Mobile)	Mp3 player (Mobile)
U+L	Page up	Scroll down	Rotate left	Volume up
U+R	Page down	Scroll up	Rotate right	Volume down
D+L	Alt + ← (back key)	Last line	Last page	First music
D+R	Alt + → (go key)	First line	First page	Last music
R+U	Ctrl + C	Next 10 pages	Next 10 pages	Next 2 music
R+D	Ctrl + V	Next page	Next Page	Next music
L+U	Ctrl + X	Previous 10 pages	Previous 10 pages	Previous 2 music
L+D	Ctrl + Z	Previous page	Previous page	Previous music

Table 3

Set commands according to applications (Level 3).

Application name	Desktop application	Text viewer, web viewer (Mobile)	Manga viewer, video viewer, gallery viewer (Mobile)	Mp3 player (Mobile)
U10	Page up	Scroll up	Rotate left	Volume up
U20	Ctrl + C	Scroll 10 line up	Upside up	Volume 10 up
U30	Home	First line	Auto page turnover On/Off	Screen On/Off
D10	Page down	Scroll down	Rotate right	Volume down
D20	Ctrl + V	Scroll 10 lines down	Upside down	Volume 10 down
D30	End	Last line	Original size/Screen fit	Shuffle On/Off
R10	Windows key + Right	Next page	Next page	Next music
R20	Ctrl + X	Next 10 pages	Next 10 pages	Next 2 music
R30	Alt + → (go key)	Last page	Last page	Last music
L10	Windows key + Left	Previous page	Previous page	Previous music
L20	Ctrl + Z	Previous 10 pages	Previous 10 pages	Previous 2 music
L30	Alt + ← (back key)	First page	First page	First music

not easy to move the eyeball in this manner. Additionally, when moving both eyeballs simultaneously, noise was generated due to interference from both eyeballs (Paul et al., 2014; Barbara et al., 2016). Therefore, we used multi-level step-wise control to improve usability while maintaining linearity in the EOG signals. Finally, the set commands of the desktop application are defined in Tables 1–3 in Section 6.2.

5. Mobile application controlling a human-computer interface using an EOG signal

5.1. Mobile application architecture

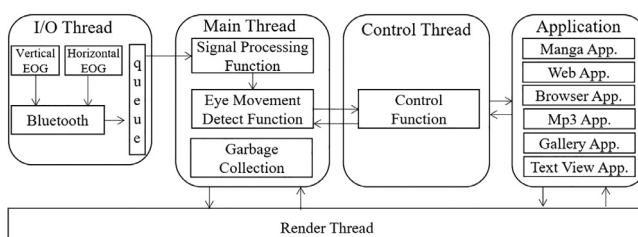
The design of the mobile application architecture (Fig. 11) is similar to that of the desktop application. Mobile devices have lower performance and less memory than desktop devices. Therefore, optimization was performed by separating the threads. The mobile application was developed based on the Android development kit and Eclipse Juno. To improve performance and memory

efficiency, the application was composed of four threads (I/O, main, control, and render) and multimedia applications. The I/O thread managed the input EOG signal and connected the EOG signal acquisition device and the mobile device via Bluetooth. The main thread controlled the other threads and managed the memory using a garbage collector, EOG signal processing, and eye movement detection. The control thread issued commands to control the application. The render thread managed the view component, as well as other components.

5.2. Mobile application

The mobile application implemented seven functions for multimedia control in the mobile device, using EOG signals. In addition, the application had an eye-protect function that displayed an alarm when the blinking rate per minute was insufficient. Fig. 12 shows screen shots of the application. The default start motion was set to double blink. The setting function was implemented in the same manner as the desktop application. The setting values were stored on an SD card. The MP3 player function could be activated as a background service. The operation was the same as that of the PC. Fig. 13 shows an example of controlling the comic viewer function by using Level 1 commands.

After execution of the start motion (double blink), the application accesses the previous page when it detects a left saccade of 30° and returns (0°), and to the next page when it detects a right saccade of 30° and returns (0°). Lastly, the set commands of the mobile application are defined in Tables 1–3 in Section 6.2. In addition, we use the developed mobile application in Sections 6.5 and 6.6.

**Fig. 11.** Mobile application architecture.

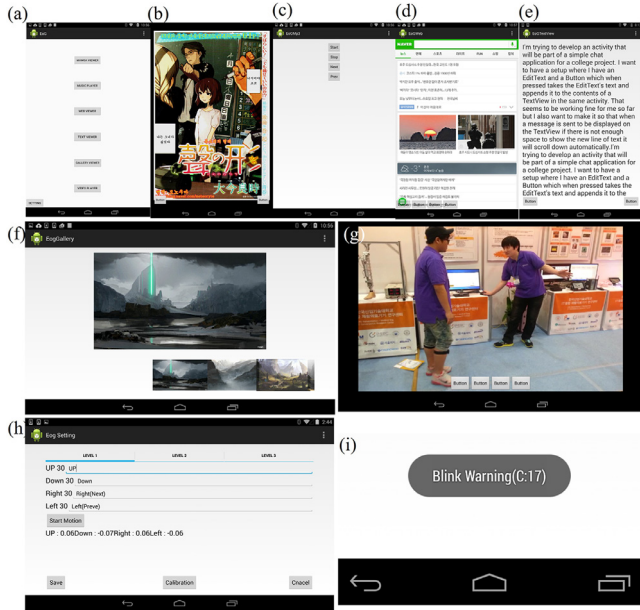


Fig. 12. Screen shots of the Android app: (a) main screen, (b) comic viewer, (c) MP3 player (service), (d) web viewer, (e) text viewer, (f) gallery viewer, (g) video viewer, (h) settings, and (i) eye-protect function.

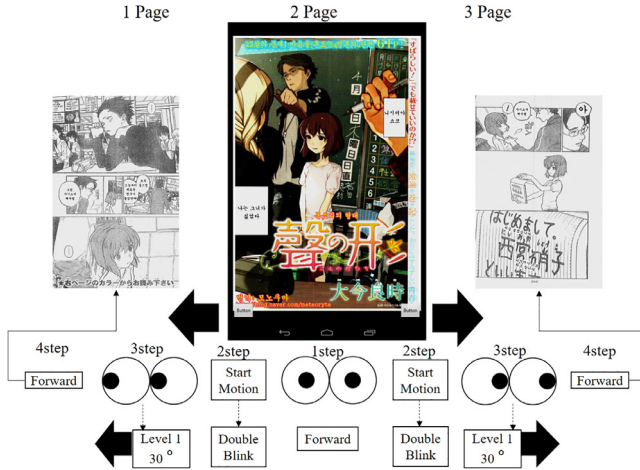


Fig. 13. Examples of controlling the comic viewer function using EOG signals and Level 1 commands.

6. Experiment and discussion

6.1. Apparatus

A commercial wireless EOG acquisition device MP150, with BioPac 2-channel BN-EOG2 Bluetooth modules, connected through the attached EOG electrodes, was used to amplify and filter the vertical and horizontal EOG signals with a 1 kHz sample rate. In addition, the MP150 was equipped with a hardware notch filter (50/60 Hz) and BPF (0.005–100 Hz) for denoising EOG signals. The EOG electrode used was wet and less sensitive to noise. The wires had already been fixed before the experiment to minimize the production of noise from head shakes. In addition, BPF were included in the Biopac acquisition device to remove muscle noise and moving artifacts. In addition, the proposed DOSbFC method included eye movement detection to recognize noise. In the PC experiment, an Intel i7-2600K processor, Windows 7, 16 GB RAM, and a Samsung SyncMaster TA950 monitor with a width of 32 cm and height of 60 cm, were used. The distance between the monitor and subject



Fig. 14. EOG eyeglasses and electrode position scheme for subjects who do not wear eyeglasses.

was fixed at 50 cm. The desktop application was implemented in Visual Studio 2013 C#. For the mobile device experiment, a Google ASUS Nexus 7 was used, and KitKat was used as the target operating system. In both experiments, EOG signals were wirelessly transmitted to the MP150 acquisition device through the BN-EOG2 Bluetooth module connected with a pair of electrodes. The MP150 acquisition device transformed EOG signals into digital output signals and transmitted them to the mobile phone or desktop PC using a LAN cable or WiFi interface.

In addition, EOG eyeglasses were created using the frame of commercial eyeglasses and BioPac bio wire for portability and application testing. Fig. 14 shows the experimental EOG eyeglasses and electrode position scheme. The wires of the experimental EOG eyeglasses were installed inside the frame of the eyeglasses, and the electrodes were arranged according to the electrode positioning scheme for eyeglasses. To eliminate muscle noises and side effects, we can choose to enable or disable the hardware BPF (0.005–100 Hz) feature on the Biopac acquisition device.

6.2. Data acquisition and experimental design

Twenty human subjects (ten males and ten females) aged 24–32 years old participated in this experiment and their average age was 27.5 years old. Ten of the subjects wore eyeglasses, and five of the subjects had dry eye syndrome (DES). The subjects have no history of eye disease, except for DES. The subjects have provided their written informed consent prior to the experimental procedures. The experimental procedures were performed in accordance with the Declaration of Helsinki and approved by the Inha University Institutional Review Board (approval: 160909-1A).

To evaluate the long-term detection of eye movements, we measured detection accuracy as a function of the electrode positioning scheme and baseline drift removal algorithm over a period of five hours. In addition, we measured the information transfer rate (ITR) (Wu et al., 2015) and detection accuracy over a period of one month using applications according to the command levels. ITR was calculated using Eqs. (6) and (7):

$$B(p, N) = p \log_2(p) + (1 - p) \log_2\left(\frac{1 - p}{N - 1}\right) + \log_2(N) \quad (6)$$

where N is the number of commands, p is the accuracy of subjects in making decisions among N targets.

$$\text{ITR}[\text{bits/min}] = \frac{\text{Number of decisions}}{\text{Recognition time per command}} \cdot B(p, N) \quad (7)$$

The experimental process of measuring the performance of the baseline drift removal algorithm ([Section 6.3](#)) and electrode positioning scheme ([Section 6.4](#)) was composed of four steps. The first step was the attachment of the electrodes. The electrodes were attached to each subject using the proposed positioning or standard positioning scheme. Each positioning scheme was performed alternately with three-day intervals, considering the subject's fatigue. The second step is the calibration to calculate the user-specific voltage as described in [Section 3](#). The third step was the eye movement detection using the desktop application. When the monitor displays a target letter randomly, the subject will gaze at it and then the eye movement is detected by the EOG signals. The experimental procedure was composed of 13 eye movements according to the eye's gaze (left (L) L10, L20, L30, right (R) R10, R20, R30, up (u) U10, U20, U30, down (d) D10, D20, D30, and blink) ([Yu et al., 2012](#); [Bulling et al., 2009](#); [Barea et al., 2002](#); [Ianez et al., 2012, 2013](#); [Liang et al., 2015](#); [Manabe et al., 2015](#); [Yamagishi et al., 2006](#); [Kirbis & Kramberger, 2009](#); [Estrany et al., 2008](#); [Yagi et al., 2006](#)). In addition, all eye movements are repeated ten times. Lastly, the fourth step repeats the third step once per hour over the five-hour period. Note that 1300 eye movements for each subject were performed (13 eye gazes \times 10 (commands) \times 5 (repetitions) \times 2 (positioning schemes)). After executing the command, the direction of the eyeball returns to the center.

Next, we evaluated the accuracy and ITR using applications according to the control commands over a period of one month (in [Sections 6.5](#) and [6.6](#), respectively). The experiment was conducted three times each week for a total of four weeks. This experiment consisted of three steps. The first and second steps were the same as those of a previous experiment. Finally, the third step was the eye movement detection using the desktop and mobile applications. The experiment was conducted over four hours using the applications, as follows: desktop application for 50 min, 10-min break, mobile application for 20 min, followed by a 10-min break. In this experiment, each subject performed eye movement actions to generate at least 1300 commands. After the subject executed the command, the supervisor or subject checked the detection error directly to determine whether an error or erroneous command had been executed. [Tables 1–3](#) show the set commands of command levels 1, 2, and 3 according to the eye movements with respect to various applications. This experiment repeated these steps a total of 12 times in one month (three times each week).

In addition, to compare across these results, baseline drift removal algorithms using hardware BPF (0.1–10 Hz) ([Yu et al., 2012](#); [Barea et al., 2002](#); [Manabe et al., 2015](#)) and Wavelet ([Bulling et al., 2011, 2009](#); [Yagi et al., 2006](#)) were implemented. In the case of wavelet, noise was removed by a software median filter while the proposed DOSbFC disables the hardware BPF and was generated by using input signal. When we compared their performance with the proposed method, these methods were applied on an already-acquired signal. However, as shown in PC and mobile applications in [Figs. 11](#) and [12](#), the DOSbFC method can be used in real-time application.

[6.3. Accuracy of long-term eye movement detection according to DC drift removal algorithms](#)

This experiment was repeated five times over five hours. Calibration was performed once at the beginning. For verifying the multi-level stepwise control scheme, at first, the accuracy of ocular movement detection using [Eq. \(2\)](#) was statistically analyzed. F statistic provides a test for the statistical significance of the performance difference of the observed saccade detection over the user-specific voltage of 5°. p is the probability that the null hypothesis - in this case, that the performance of observed saccade detection doesn't vary by the user-specific voltage of 5°. According

to the one way analysis of variance, the accuracy of ocular movement detection using [Eq. \(2\)](#) was significant ($F=7.28$, $p < 0.01$). In many studies, the EOG signal guarantees linearity up to 30° ([Simini et al., 2011](#), [Webster, 1998](#)). Therefore, the saccades detection range in [Eqs. \(4\)](#) and [\(5\)](#) was limited to 30° (+−5) to minimize the linearity error of the EOG signal. The accuracy of eye movement detection using [Eqs. \(4\)](#) and [\(5\)](#) was statistically analyzed. F statistic provides a test for the statistical significance of the performance difference of the observed gaze angle of saccade movement over the amplitude of the signal. p is the probability that the null hypothesis - in this case, that the performance of observed gaze angle of saccade movement doesn't vary by the amplitude of the signal. The ANOVA results demonstrated that the accuracy of up/down saccade eye movement detection using [Eq. \(4\)](#) was significant ($F=5.81$, $p < 0.01$) and that of left/right saccade eye movement detection using [Eq. \(5\)](#) was significant ($F=4.36$, $p < 0.01$).

[Fig. 15\(a\)](#) shows the accuracy of long-term eye movement detection with respect to BPF, wavelet, and DOSbFC, respectively. The results demonstrate that the accuracy of the eye-movement detection for the proposed method was higher than for BPF and wavelet, as determined from an analyses of variation in time and eye movements. The average accuracies for BPF, wavelet, and DOSbFC were 63%, 64%, and 94%, respectively. [Fig. 15\(b\)](#) shows the average true positive rate, true negative rate, false positive rate, and false negative rate of long-term eye movement detection with respect to BPF, wavelet, and DOSbFC, respectively. False alarms, as the average of rates of false positive and false negative rate, of BPF and wavelet were 37.3% and 35.5% whereas that of the DOSbFC was 6.3%. In addition, the true positive rate and true negative rate of the DOSbFC were 95%, and 92.4% respectively. The DOSbFC separated true and false datasets better than existing methods.

[Fig. 15\(c\)](#) shows that the three methods had similar accuracies during the first hour. One-way analysis of variance demonstrated that the variation in accuracy of the first one hour was not significant ($F=0.42$; $P > 0.01$). However, after one hour, the standard deviation in the accuracy for BPF and wavelet increased to 24% owing to severe baseline drift, whereas the proposed DOSbFC method had a uniform performance with a standard deviation of 4%. One-way analysis of variance demonstrated that variation (ANOVA) in accuracy after first one hour was significant ($F=23.63$; $p < 0.01$). The accuracy of the proposed DOSbFC method was higher than that for existing methods ([Fig. 15\(a\)](#)).

Analysis of the experimental results showed that the accuracy of detection of eye movements of 30° in each direction was higher than that for other angles, for all algorithms. In contrast, eye movement of 20° in all directions showed the lowest detection accuracy. Replication of maximum and minimum eye movements was easy for all subjects they found reproduction of the middle eye movement of 20° difficult. All subjects commented “20° are somewhat difficult to reproduce”. [Fig. 16](#) shows the converted signals of the BPF, wavelet, and DOSbFC methods when linear baseline drift had occurred. This demonstrated the occurrence of horizontal EOG signals when a subject repeated the same eye movement five times, such as “looking at a spot located 30° right on the screen”, and “looking at a spot located 30° left on the screen”. Our results showed that the baseline of EOG signals for both BPF and wavelet shifted 10–20° from the zero voltage, whereas the baseline for the DOSbFC method is proximal to zero volts. This is because the proposed baseline drift removal method used averaged signal variation. In addition, the DOSbFC method converted EOG signals to a relative ocular displacement of eye movement using the difference equation, shown in [\(1\)](#). The DOSbFC algorithm is a signal conversion method that used the relationship between the activation of a neuron and fixation time. In addition, the proposed method increased accuracy because it is a baseline drift removal algorithm that combined widely used BPF, moving average and differential

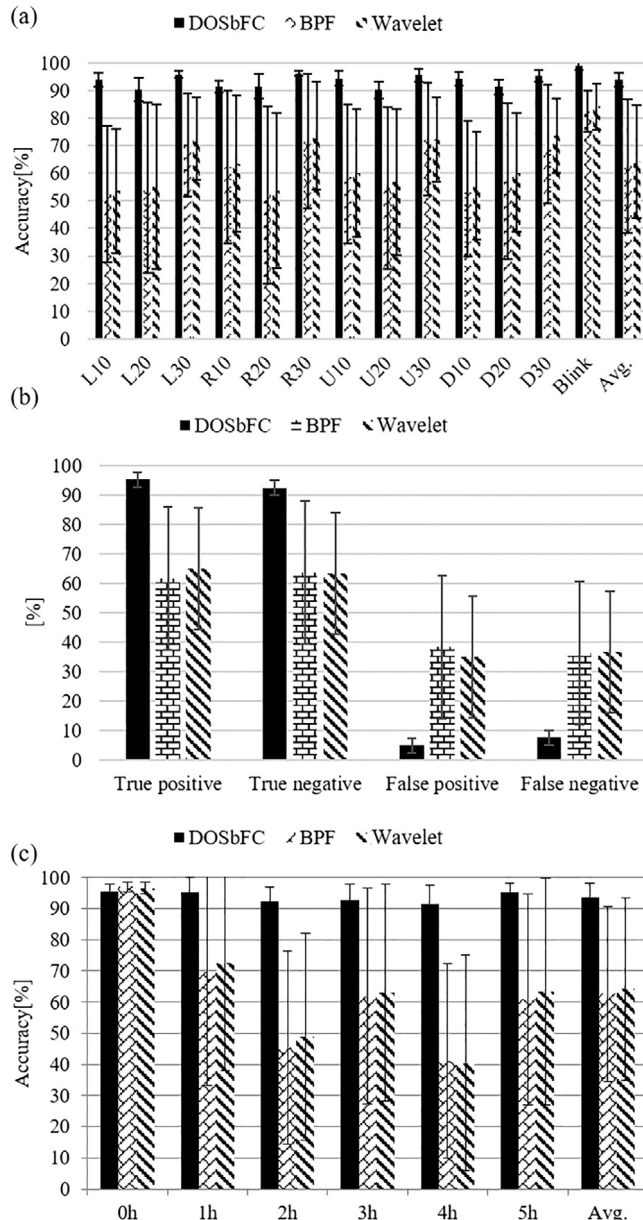


Fig. 15. Evaluation of the long-term eye movement detection according to the DC drift removal algorithms: (a) accuracy according to the eye movements, (b) average true positive rate, true negative rate, false positive rate, and false negative rate according to the eye movements, and (c) accuracy according to time.

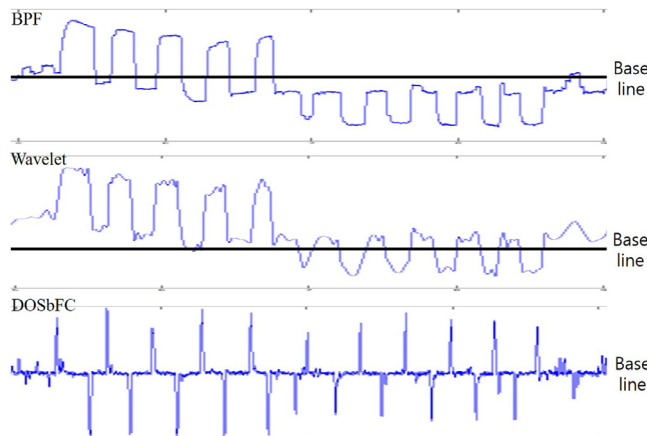


Fig. 16. Converted signals after baseline drift (BPF is raw input signal).

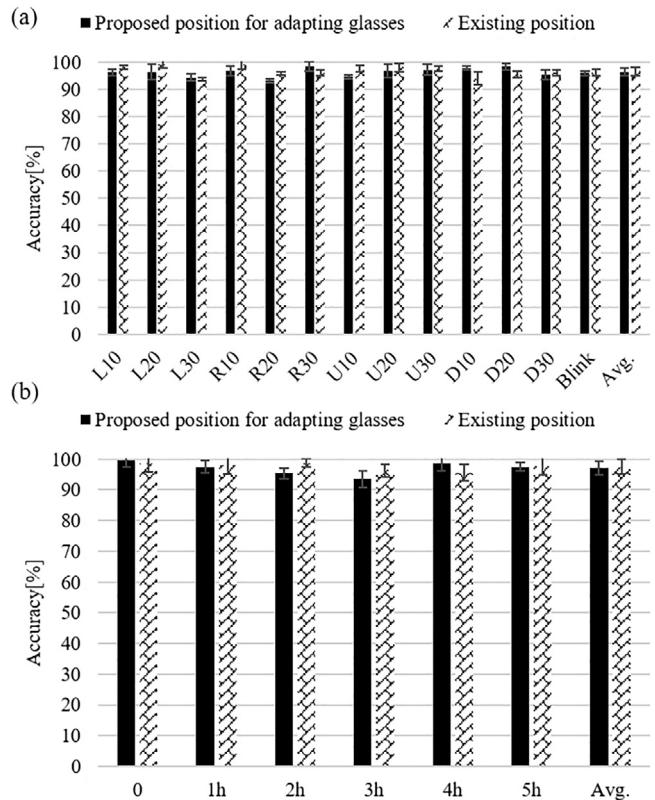


Fig. 17. Evaluation of long-term eye movement detection according to the electrode positioning scheme over five hours: (a) accuracy according to the eye movements and (b) accuracy according to time.

equations. Therefore, the DOSbFC method remained unaffected by a gradually varying baseline drift, whereas existing baseline drift removal algorithms are affected as they use the absolute position of eye movement.

6.4. Accuracy with reference to the electrode positioning scheme

This experiment used a baseline drift removal algorithm of the DOSbFC method. Fig. 17 shows the evaluation of long-term eye movement detection according to the electrode positioning scheme, over a period of five hours. The accuracies of the proposed positions were the same as those of the standard positions with respect to various eye movements. The average accuracies of the proposed and standard positioning schemes were 97.5% and 97%, respectively. ANOVA demonstrated that the variation in accuracy of the positioning scheme was not significant ($F=0.48$; $P > 0.01$).

The accuracy of the proposed positioning scheme to adapt eyeglasses, and the standard positioning scheme were similar in terms of the time change and eye movements. Both eyeballs of a normal subject move simultaneously in the same direction. Therefore, changing the electrode attachment position did not affect the linearity of the EOG signals as the electrodes of the proposed method were located between the eyes, similar to the electrode position of the horizontal EOG signals. In addition, all subjects commented that the proposed positioning scheme was more comfortable than the standard positioning scheme, and they support the commercialization of the EOG eyeglasses using the proposed electrode position scheme.

In the usability evaluation, 20 subjects commented that the proposed positioning scheme was more useful and convenient than the standard positioning scheme. In the case of the standard positioning scheme, when electrodes are attached for more than 1 h, all subjects experienced discomfort in the lower vertical electrodes,

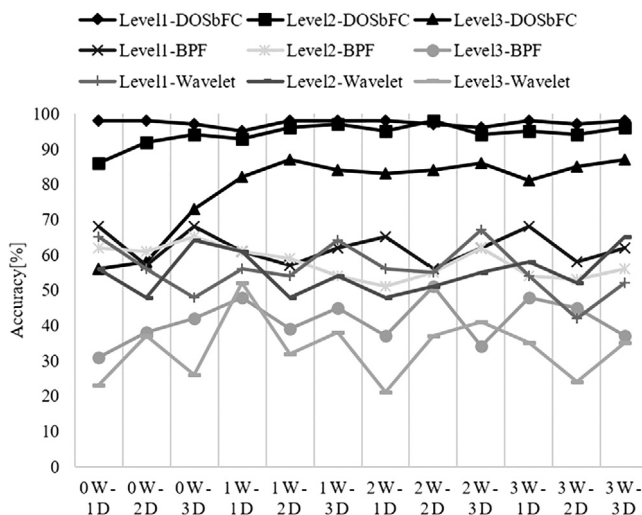


Fig. 18. Detection accuracy of long-term eye movements using the applications according to the command levels over four weeks.

and some subjects had fine seizures due to the weight of the electrodes. In addition, ten subjects wearing eyeglasses complained of the discomfort due to the interference of the vertical electrodes with the glasses frame whereas the proposed positioning scheme made subjects feel more comfortable because the electrode was attached to the nasal skeleton.

6.5. Accuracy using applications as a function of command levels

The ITR has commonly been used to assess the performance of human-machine interface systems. The ITR is calculated using recognition time per command including processing time, and detection accuracy as important factors. In this experiment, we evaluated the accuracy of long-term eye movement detection using the proposed method and applications as a function of command levels over a four-week period. This experiment was performed to evaluate the effectiveness of the command levels as user proficiency increased.

Fig. 18 shows that the proposed method improved the detection accuracy with increasing proficiency. In particular, at all command levels, the accuracy of the proposed DOSbFC method increased and maintained its status as the most accurate after a period of 1 week (W) - 2 days (D). In contrast, as shown in Section 6.3, the detection accuracies using the existing methods were lower than 70% owing to baseline drift. For Level 3, the proposed method exhibited a detection accuracy lower than 70% until 0W-2D. Subjects reported initial difficulty in reproducing the 20° position for all directions at Level 3. However, the detection accuracy of the DOSbFC method at Level 3 improved to 87% when the experiment was conducted for more than 16 h at 1W-2D. Therefore, accurate detection of eye movements at Level 3 required more than 16 h of training. The average detection accuracy of DOSbFC at Levels 1 and 2 were 98% and 86%, respectively, when evaluated at 0W-1D. The subjects were able to reproduce eye movements easily at Levels 1 and 2. This is due to the commands being generated with eye movements over 30°. For Levels 1 and 2, the eye movement accuracies using the DOSbFC method after 0W-1D (Level 1) and 0W-2D (Level 2) remained the highest. The command generation at Level 1 does not require any training, whereas the command generation at Level 2 required a training period of more than four hours.

6.6. ITR using application according to command levels

In this experiment, we evaluated the ITR of command levels using the proposed method and application. We called subjects who

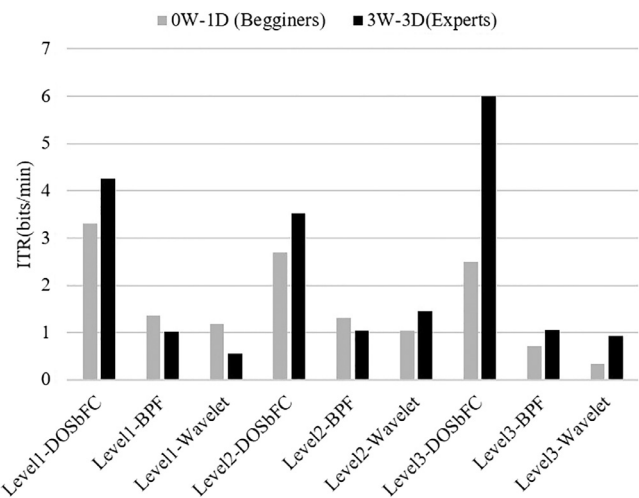


Fig. 19. ITR of long-term eye movement detection using applications according to the command levels.

lack the skills to generate command levels "beginners," and subjects who possessed the skills to generate command levels "experts." We calculated the ITR of command levels using the experimental results over 0W-1D and 3W-3D to compare the efficiency of the beginners and experts. In other words, 0W-1D denotes the experimental result using the beginners, and 3W-3D denotes the experimental result using the experts.

Fig. 19 shows the ITR of long-term eye movement detection using applications according to the command levels.

Our results show that the ITR of eye-movement detection using the proposed methods was higher than that of the BPF and wavelet methods, depending on the command levels. The average ITR at 0W-1D for BPF with Level 1, Level 2, and Level 3; wavelet with Level 1, Level 2, and Level 3; and DOSbFC with Level 1, Level 2, and Level 3 were 1.4, 1.3, 0.7, 1.2, 1.0, 0.3, 3.3, 2.7, and 2.5, respectively. In addition, the average ITR of 3W-3D for BPF with Level 1, Level 2, and Level 3; wavelet with Level 1, Level 2, and Level 3; and DOSbFC with Level 1, Level 2, and Level 3 were 1.0, 1.0, 1.1, 0.5, 1.4, 0.9, 4.2, 3.5, and 6.0, respectively. For 0W-0D, Level 1 showed an overall high average ITR. Even beginner subjects were able to generate commands as well as the expert subjects as Level 1 simply involved generating commands using four directions. The Level 2 and 3 tests resulted in a lower accuracy of eye movements and ITR among beginners than that of Level 1 owing to lack of training time. For 3W-3D, then ITR at Level 3 was increased significantly. This was because the subject had received sufficient training to generate commands easily and with greater accuracy. Level 3 allowed the generation of 12 commands simultaneously, whereas at Level 1, only four commands could be generated at once. In addition, all subjects preferred Level 1 for simple operations and Level 3 for complex operations. Therefore, our results showed that the proposed method had a higher ITR than existing methods, and that it was the best method to use at Level 1, for simple operations, as well as at Level 3 for complicated operations because the DOSbFC had a higher accuracy and faster detection time than existing method.

7. Conclusion

This paper proposed a new electrode positioning scheme based on eyeglasses and a new baseline drift and noise removal method called DOSbFC. The experimental results showed that the average accuracy of long-term eye movement detection using the DOSbFC was 94%, whereas that using a BPF and wavelet transform was 61% and 64%, respectively. It was demonstrated that DOSbFC

can separate true and false datasets more accurately than existing methods. In addition, the results of one-way analysis of variance showed that differences in performance between existing methods and the proposed method was significant. In contrast, differences arising from the proposed positioning scheme and the standard positioning scheme were not significant. The proposed method had less or no difference in throughput because it was based on moving average and differential equations for use on mobile devices. We used snap dragon S4 Pro in the experiment, but the proposed method worked well and showed higher ITR than existing methods.

In addition, a desktop application for PC control and a mobile application for mobile device control were implemented. Lastly, we created experimental EOG eyeglasses using the proposed method to aid long-term detection of eye movements and subject convenience. In an evaluation of usability, 20 subjects commented that the proposed positioning scheme was more useful and convenient than the standard positioning scheme.

The contributions of the proposed method are as follows: it can remove baseline drift and noise effectively; it provides a long-term eye-tracking function with high accuracy in activity recognition; and it provides higher ITR than existing methods.

In future studies, we aim to improve portability by manufacturing ergonomic EOG eyeglasses using dry electrodes and an EOG signals acquisition board based on microelectromechanical systems. In addition, in this study, we proposed a baseline drift removal and denoising algorithm for static motion. Therefore, we will study algorithms for dynamic motion in the future. In addition, we did not consider diagonal and over 35° saccade for computation speed and detection error rate. The maximum eye movement range of an individual is approximately 45°. In addition, interference noise occurs when vertical and horizontal saccades are performed simultaneously. In future studies, we will develop algorithms that can extend detection range and recognize diagonal motion. Lastly, our DOSbFC is optimized for step-by-step eye movement because it aims at command recognition. Therefore, it is not suitable for pursuits requiring smooth eye movements, such as reading. In future studies, we will develop an absolute displacement eye recognition algorithm using baseline correction based on DOSbFC.

The proposed method can be extended to different tasks, such as human motion recognition and human and robot system activity analysis, using EOG signals. In addition, the proposed method is expected to be usable as a fundamental method for solving baseline drift of bio signals without the need for a reference signal. Finally, the proposed method is expected to be useful not only for rehabilitation areas such as paralysis patients and upper limb amputees, but also as a base technology for generation of command signals to assist workers in an environment where hands are difficult to use.

Acknowledgements

This research was supported in part by the Basic Science Research Program through the National Research Foundation of Korea funded by the Ministry of Education (2018R1D1A1B07042602, 2010-0020163) and in part by the Industrial Technology Innovation Program funded by the Ministry of Trade, Industry & Energy (MI, Korea) [10073154, Development of human-friendly human-robot interaction technologies using human internal emotional states].

Conflicts of interest

The authors declare that no conflicts of interest exist.

References

- Barbara, N., & Camilleri, T. A. (2016). Interfacing with a speller using EOG glasses. In *Proc. 2016 IEEE international conference on systems, man, and cybernetics (SMC)*. doi:10.1109/SMC.2016.7844384.
- Barbara, N., Camilleri, T. A., & Camilleri, K. P. (2019). EOG-based eye movement detection and gaze estimation for an asynchronous virtual keyboard. *Biomedical Signal Processing and Control*, 47, 159–167. doi:10.1016/j.bspc.2018.07.005.
- Barea, R., Boquete, L., Mazo, M., & Lopez, E. (2002). Wheelchair guidance strategies using EOG. *Journal of Intelligent and Robotic Systems*, 34(July(3)), 279–299. doi:10.1023/A:101635950.
- Barea, R., Boquete, L., Roteaga, S., Lopez, E., & Rodriguez-Ascariz, J. M. (2012). EOG-based eye movements codification for human computer interaction. *Expert Systems with Applications*, 39(February(3)), 2677–2683. doi:10.1016/j.eswa.2011.08.123.
- Blehm, C., Vishnu, S., Khattak, A., Mitra, S., & Yee, R. W. (2005). Computer vision syndrome: A review. *Survey of Ophthalmology*, 50(June(3)), 253–262. doi:10.1016/j.survophthal.2005.02.008.
- Brown, M., Marmor, M., Vaegan, V., Zrenner, E., Brigell, M., & Bach, M. (2006). IS-CEV standard for clinical electro-oculography (EOG). *Documenta Ophthalmologica*, 113(November(3)), 205–212. doi:10.1007/s10633-006-9030-0.
- Bulling, A., Roggen, D., & Troster, G. (2009). Wearable EOG goggles: seamless sensing and context-awareness in everyday environments. *Journal of Ambient Intelligence and Smart Environments*, 1(2), 157–171. doi:10.3233/AIS-2009-0020.
- Bulling, A., Ward, A., Gellersen, H., & Troster, G. (2011). Eye movement analysis for activity recognition using electrooculography. *IEEE Transactions on Pattern Analysis and Machine Intelligence*, 33(4), 741–753. doi:10.1109/TPAMI.2010.86.
- Chouhan, V. S., & Mehta, S. S. (2007). Total removal of baseline drift from ECG signal. In *Proc. IEEE international conference on computing: theory and application* (pp. 512–515). doi:10.1109/ICCTA.2007.126.
- Deng, L. Y., Hsu, C. L., Lin, T. C., Tuan, J. S., & Chang, S. M. (2010). EOG-based human-computer interface system development. *Expert Systems with Applications*, 37(October(4)), 3337–3343. doi:10.1016/j.eswa.2009.10.017.
- Deseilligny, C. P., Muri, R. M., Ploner, C. J., Gaymard, B., & Pechoux, S. R. (1995). Cortical control of saccades. *Annals of Neurology*, 37(May(5)), 557–567. doi:10.1002/ana.410370504.
- Draper, S. (2018). Imec's wireless eye-tracking glasses will help research neurological disorders. *Wearable Technologies Europe*. Retrieved Jun. 7, 2018, from <https://www.wearable-technologies.com/2018/06/imecs-wireless-eye-tracking-glasses-will-help-research-neurological-disorders/>.
- Estrany, B., Fuster, P., Garcia, A., & Luo, Y. (2008). Human computer interface by EOG tracking. In *Proc. ACM international conference on pervasive technologies related to assistive environments*: 96 (pp. 1–96). 9. doi:10.1145/1389586.1389694.
- Fernandez, J. M., Augusto, J. M., Seepold, R., & Madrid, N. M. (2012). A sensor technology survey for a stress-aware trading process. *IEEE Transactions on Systems, Man, and Cybernetics-Part C: Applications and Reviews*, 42(November(6)), 809–824. doi:10.1109/TSMCC.2011.2179028.
- Harun, H., & Mansor, W. (2009). EOG signal detection for home appliances activation. In *Proc. IEEE intl. conference on CSPA* (pp. 195–197). doi:10.1109/CSPA.2009.5069215.
- Huaman, A. G., & Sharpe, J. A. (1993). Vertical saccades in senescence. *Investigative Ophthalmology & Visual Science*, 34(July(8)), 2588–2595.
- Kirbis, M., & Kramerberger, I. (2009). Mobile device for electronic eye gesture recognition. *IEEE Transactions on Consumer Electron.*, 55(November(4)), 2127–2133. doi:10.1109/TCE.2009.5373778.
- Kunze, K., & Tanaka, K. (2014). Smarter eyewear- using commercial EOG glasses for activity recognition. In *Proc. UbiComp' 14 Adjunct* (pp. 239–242). pp.. doi:10.1145/2638728.2638795.
- Ianez, E., Azorin, J. M., & Perez-vidal, C. (2013). Using eye movement to control a computer: A design for a lightweight electro-oculogram electrode array and computer interface. *PLOS ONE*, 8(July(7)), e67099 volno.. doi:10.1371/journal.pone.0067099.
- Ianez, E., Ubeda, A., Azorin, J. M., & Perez-vidal, C. (2012). Assistive robot application based on an RFID control architecture and a wireless EOG interface. *Robotics and Autonomous Systems*, 60(August(8)), 1069–1077. doi:10.1016/j.robot.2012.05.006.
- Liang, S., Kuo, C., Lee, Y., Lin, W., Liu, Y., Chen, P., et al. (2015). Development of an EOG-based automatic sleep-monitoring eye mask. *IEEE Transactions on Instrumentation and Measurement*, 64(November(11)), 2977–2985. doi:10.1109/TIM.2015.2433652.
- Manabe, H., Fukumoto, M., & Yagi, T. (2015). Direct gaze estimation based on nonlinearity of EOG. *IEEE Transactions on Biomedical Engineering*, 62(June(6)), 1553–1562. doi:10.1109/TBME.2015.2394409.
- Merino, M., Rivera, O., Gómez, I., Molina, A., & Dorronzoro, E. (2010). A method of EOG signal processing to detect the direction of eye movements. In *Proc. intl. conference on sensor device technologies and applications*. doi:10.1109/SENSORDEVICES.2010.25.
- Paul, G. M., Cao, F., Torah, R., Yang, K., Beeby, S., & Tudor, J. (2014). A smart textile based facial EMG and EOG computer interface. *IEEE Sensors Journal*, 14(February), 393–400.
- Postelnicu, C., Girbacia, F., & Talaba, D. (2012). EOG-based visual navigation interface development. *Expert Systems with Applications*, 39(September(12)), 10857–10866. doi:10.1016/j.eswa.2012.03.007.
- Rahman, M. M., Bhuiyan, M. I. H., & Hassan, A. R. (2018). Sleep stage classification using single-channel EOG. *Computers in Biology and Medicine*, 102(August(1)), 211–220. doi:10.1016/j.combiomed.2018.08.022.

- Riggs, L. A., Kelly, J. P., Manning, K. A., & Moore, R. K. (1987). Blink-related eye movements. *Investigative Ophthalmology & Visual Science*, 28(February), 334–342.
- Simini, F., Touya, A., Senatore, A., & Pereira, J. (2011). Gaze tracker by electrooculography (EOG) on a head-band. In *Proc. 2011 IEEE international workshop on biomedical engineering*. doi:[10.1109/IWBE.2011.6079050](https://doi.org/10.1109/IWBE.2011.6079050).
- Tinati, M. A., & Mozaffary, B. (2006). A wavelet packets approach to electrocardiograph baseline drift cancellation. *International Journal of Biomedical Imaging*, 2006 vol. 9. doi:[10.1155/IJBI/2006/97157](https://doi.org/10.1155/IJBI/2006/97157).
- Webster, J. G. (1998). *Medical instrumentation: application and design*. John Wiley and Sons.
- Wu, J. F., Ang, A. M. S., Tsui, K. M., Wu, H. C., Hung, Y. S., Hu, Y., et al. (2015). Efficient implementation and design of a new single-channel electrooculography-based human-machine interface system. *IEEE Transactions on Circuits and Systems*, 62(February(2)), 179–183. doi:[10.1109/TCSIL.2014.2368617](https://doi.org/10.1109/TCSIL.2014.2368617).
- Wu, S. L., Liao, L. D., Lu, S. W., Jiang, W. L., Chen, S. A., & Lin, C. T. (2013). Controlling a human-computer interface system with a novel classification method that uses electrooculography signals. *IEEE Transactions on Biomedical Engineering*, 60(August (8)), 2133–2141. doi:[10.1109/TBME.2013.2248154](https://doi.org/10.1109/TBME.2013.2248154).
- Yagi, T., Kuno, Y., Koga, K., & Mukai, T. (2006). Drifting and blinking compensation in electro-oculography (EOG) eye-gaze interface. In *Proc. IEEE international conference on systems, man and cybernetics* (pp. 3222–3226). doi:[10.1109/ICSMC.2006.384613](https://doi.org/10.1109/ICSMC.2006.384613).
- Yamagishi, K., Hori, J., & Miyakawa, M. (2006). Development of EOG-based communication system controlled by eight-directional eye movements. In *Proc. IEEE international conference on EMBS* (pp. 2574–2577). doi:[10.1109/IEMBS.2006.259914](https://doi.org/10.1109/IEMBS.2006.259914).
- Yao, W., Davidson, R. S., Durairaj, V. D., & Gelston, C. D. (2011). Dry eye syndrome: an update in office management. *The American Journal of Medicine*, 134(November(11)), 1016–1018. doi:[10.1016/j.amjmed.2011.01.030](https://doi.org/10.1016/j.amjmed.2011.01.030).
- Yu, J. H., Lee, B. H., & Kim, D.-H. (2012). EOG based eye movement measure of visual fatigue caused by 2D and 3D displays. In *Proc. IEEE-EMBS international conference on BHI* (pp. 305–308). doi:[10.1109/BHI.2012.6211573](https://doi.org/10.1109/BHI.2012.6211573).
- Zhang, J., Yin, Z., & Wang, R. (2015). Recognition of mental workload levels under complex human-machine collaboration by using physiological features and adaptive support vector machines. *IEEE Transactions on Human-Machine Systems*, 45(2), 200–214. doi:[10.1109/THMS.2014.2366914](https://doi.org/10.1109/THMS.2014.2366914).